Structural Analysis of Historical Constructions, New Delhi 2006
P.B. Lourenço, P. Roca, C. Modena, S. Agrawal (Eds.)

# Structural Characterization of Rakanji Stone Arch Bridge by Numerical Model Updating

T. Aoki
*Nagoya city University, Graduate school of Design and Architecture, Nagoya, Japan*

D. Sabia and D. Rivella
*Polytechnic of Turin, Department of Structural and Geotechnical Engineering, Turin, Italy*

T. Komiyama
*Constec Engineering Co., Ltd., Osaka, Japan*

ABSTRACT: The Rakanji stone arch bridge has three spans of about 26 m, and the total length of the bridge is about 89.3 m. The rise span ratio is about 0.19; hence, the arches are very shallow. In order to clarify the structural characterization of the Rakanji stone arch bridge, a series of dynamic, non-destructive and destructive tests are carried out. From the results of dynamic tests, the fundamental frequencies of the Rakanji stone arch bridge are estimated to be about 5.3 Hz and 7.6 Hz in the out-of-plane and vertical directions, respectively. Its natural modes are identified by ERA (eigensystem realization algorithm) model. From the results of numerical model updating based on IEM (inverse eigensensitivity method), a reliable numerical model which can simulate the real behaviour of the Rakanji arch bridge is obtained.

## 1 INTRODUCTION

The construction of the Rakanji stone arch bridge over the Yamakuni River, Honyabakei, Oita, started in 1917; it was supervised by Shinnosuke MATSUDA and Mankichi IWABUCHI, famous engineers in the construction field during this period (Fig. 1). During construction, the bridge had collapsed twice before its completion in 1920. It has three spans of about 26 m, and the total length of the bridge is about 89.3 m. The rise of the stone arches is about 5.1 m, and their radical thickness is about 0.93 m. The rise span ratio is about 0.19; in other words, the arches are very shallow. The width of the bridge is about 4.5 m. The bridge has been designated as cultural property by Oita prefecture because of its grandeur, elegance and historic value.

In the previous study, various tests and measurements are carried out to evaluate the deterioration of the bridge (Aoki et al. 2004a) and experimental and theoretical dynamic analyses are performed to assess the structural stability of the Rakanji stone arch bridge (Aoki et al. 2004b). The purpose of this paper is to estimate the structural characterization of the Rakanji stone arch bridge by numerical model updating.

Figure 1 : Rakanji stone arch bridge

Table 1 : Measurement set-up for Rakanji stone arch bridge

| Setup | Channel 1 | 2 | 3 | 4 | 5 | 6 |
|---|---|---|---|---|---|---|
| 1 | 2 | 12 | 1 | 3 | 10 | 11 |
| 2 | 2 | 12 | 4 | 5 | 13 | 14 |
| 3 | 2 | 12 | 6 | 7 | 15 | 16 |
| 4 | 2 | 12 | 8 | 9 | 17 | 18 |
| 5 | 2 | 12 | 19 | 20 | 21 | 22 |

## 2 DYNAMIC TESTS

### *2.1 Microtremor measurement*

In order to obtain data on the dynamic structural properties of the Rakanji stone arch bridge, in the first phase of dynamic testing, microtremors are measured from the ambient vibrations at different points, as shown in Fig. 2. Smoothed spectra obtained using a Parzen spectral window of 0.1 Hz are presented in Fig. 3. In this figure, the fine solid line, bold dotted line and bold solid line represent the spectra of the longitudinal, out-of-plane and vertical directions, respectively. From the microtremor measurements, the fundamental frequencies of the Rakanji stone arch bridge are estimated to be 5.3 Hz and 7.6 Hz in the out-of-plane and vertical directions, respectively (Aoki et al. 2004b).

### *2.2 Acceleration measurement*

In the second phase of dynamic testing, acceleration is simultaneously measured at six points in the vertical direction. Five different set-ups are prepared at the six measuring points, as shown in Fig. 2 and Table 1. Two sensors are fixed at points 2 and 12 in Fig. 2, and the others are placed as shown in Table 1. The total number of measuring points is 22. Ground vibrations created by a truck serves as the excitation.

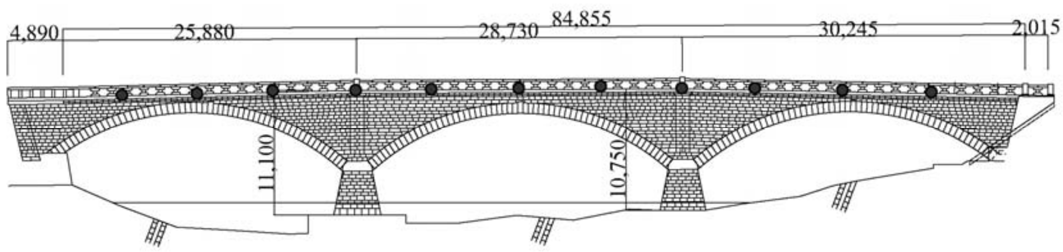


(a) Elevation of downstream side (unit: mm)

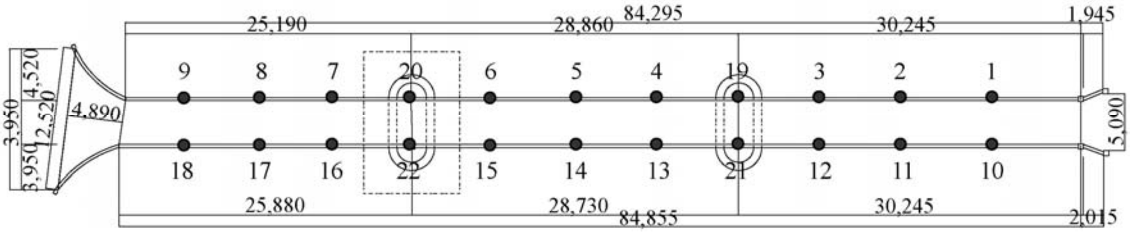


(b) Plan (unit: mm)

Figure 2 : Elevation and plan and measuring points

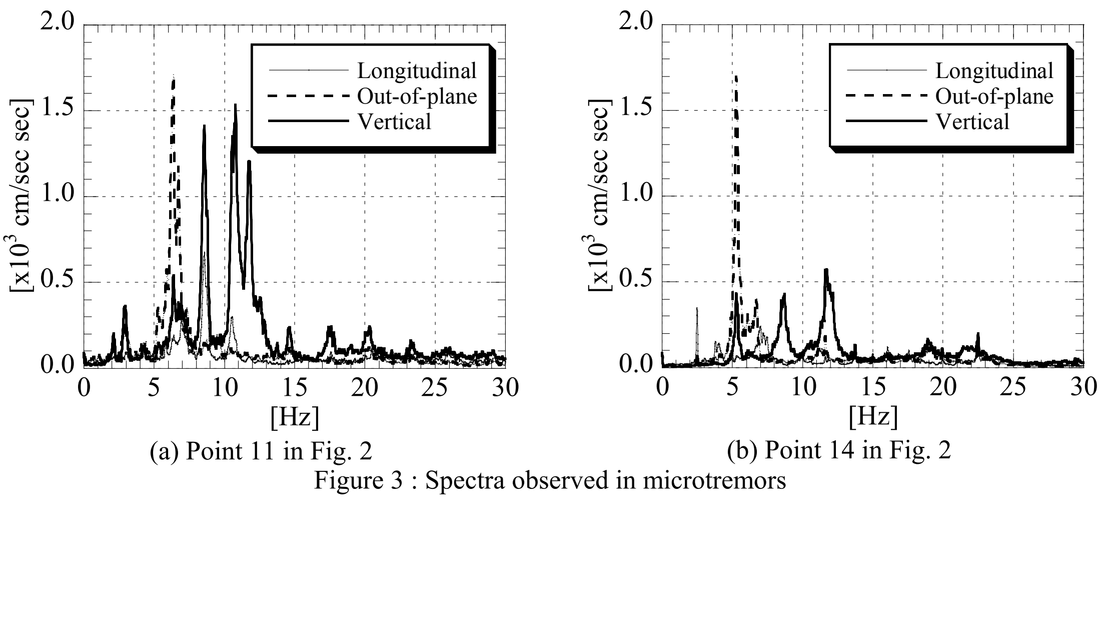


(a) Point 11 in Fig. 2 (b) Point 14 in Fig. 2

Figure 3 : Spectra observed in microtremors

## 3 DYNAMIC IDENTIFICATION

### 3.1 *ERA technique*

The ERA (eigensystem realization algorithm) model (Juang and Pappa 1985) is one of the most widely used to determine the modal parameters of a dynamic system, such as the fundamental frequencies, mode shapes and damping factors, based on the description of its behaviour in the space between the phases.

### 3.2 *Results of dynamic identification*

Fig. 4 shows the frequency distributions of the Rakanji stone arch bridge in the vertical direction, as determined by the ERA model considering the complete time record. The five experimental modes, 7.90 Hz, 9.18 Hz, 11.02 Hz, 11.89 Hz and 19.79 Hz in vertical direction, are identified (Aoki et al. 2004b).

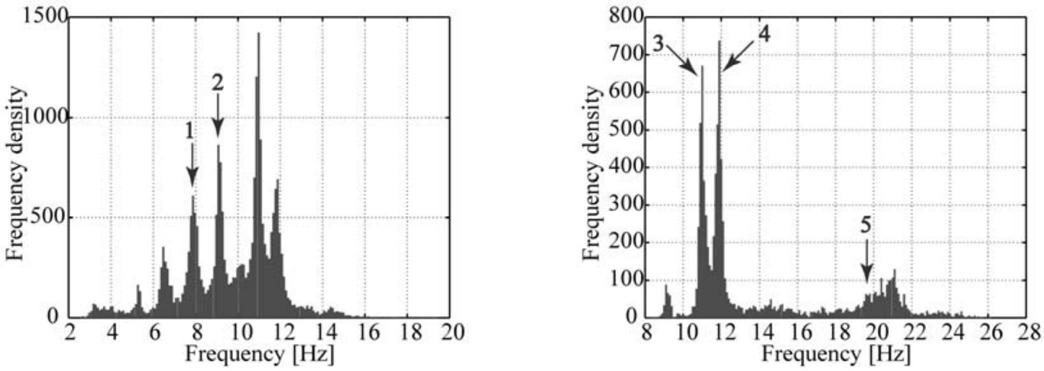


(a) 3 Hz - 11 Hz (b) 9 Hz – 26 Hz

Figure 4 : Frequency distribution identified by ERA model

## 4 NUMERICAL MODEL UPDATING

### 4.1 *Theoretical background*

Model updating aims to minimize the differences between the experimental measurements and the theoretical dynamic response of a model (Friswell and Mottershead 1995). In this section, IEM (inverse eigensensitivity method) is briefly introduced (Jung and Ewins 1992) and applied to the Rakanji stone arch bridge.

The model updating procedure is based on the computation of suitable correction coefficients $a_i$ and $b_i$; these coefficients are associated with the mass and stiffness of the *i*-th element, respectively, such that all the relations that refer to the corrected matrices of the model are satisfied as follows:

$$[M_u]=\sum_{i=1}^{L} a_i \cdot [M]_i \quad , \qquad [K_u]=\sum_{i=1}^{L} b_i \cdot [K]_i \tag{1}$$

where *L* is the number of elements or macro elements in the structure.

Matrices $[M]_i$ and $[K]_i$ are sub-matrices of the system and may correspond to the matrices of *sub-elements*, *elements* or *macro elements* (substructures).

All models that employ sensitivity-based methods are generally based on the use of expansions in the Taylor series in which mode data, which are considered as a function of unknown parameters, are truncated. The expansion in the series is frequently truncated after the first two terms, which yields a linear approximation that is expressed as follows:

$$\{\Delta w\}=[S]\cdot\{\Delta p\} \tag{2}$$

where $\{\Delta w\}=\{\Delta\lambda_1,\{\Delta\phi_1\},\ \Delta\lambda_2,\{\Delta\phi_2\},\dots,\Delta\lambda_m,\{\Delta\phi_m\}\}^T$ is the error in the measured outputs; $\Delta\lambda_i$, the error in the *i*-th eigenvalue; $\{\Delta\phi_i\}$, the error in the corresponding mode shape; $\{\Delta p\}$, the perturbation in the parameters and $[S]$, the sensitivity matrix containing the first derivatives of the eigenvalues and eigenvectors with respect to the parameters estimated in the previous iteration.

The sensitivity matrix represents the relation between the variations in the physical parameters and the error in the dynamic structural response expressed in terms of the frequencies and mode shapes.

By using a Taylor series expansion, the $r$-th eigenvalue and eigenvector contributions can be determined as follows:

$$\begin{Bmatrix} \Delta\lambda_r \\ \{\Delta\phi\}_r \end{Bmatrix} = \begin{bmatrix} \frac{\partial\lambda_{Ar}}{\partial a_1}/\lambda_{Ar} & \cdots & \frac{\partial\lambda_{Ar}}{\partial a_L}/\lambda_{Ar} & \frac{\partial\lambda_{Ar}}{\partial b_1}/\lambda_{Ar} & \cdots & \frac{\partial\lambda_{Ar}}{\partial b_L}/\lambda_{Ar} \\ \frac{\partial\{\phi_A\}_r}{\partial a_1} & \cdots & \frac{\partial\{\phi_A\}_r}{\partial a_L} & \frac{\partial\{\phi_A\}_r}{\partial b_1} & \cdots & \frac{\partial\{\phi_A\}_r}{\partial b_L} \end{bmatrix} \begin{Bmatrix} \Delta a_1 \\ \vdots \\ \Delta a_L \\ \Delta b_1 \\ \vdots \\ \Delta b_L \end{Bmatrix} \tag{3}$$

Eq. (3) can be simplified by using the vector $\{p\}$ that contains the correction coefficients $\{a_1, a_2,\ldots, a_L, b_1, b_2,\ldots, b_L\}^{\mathrm{T}}$:

$$\{\Delta_r\}_{[(n+1)\times 1]} = [S_r]_{[(n+1)\times 2L]}\{\Delta p\}_{[2L\times 1]} \tag{4}$$

where $n$ is the number of coordinates measured.

From the solution of Eq. (4), the vector $\{p\}$ can be determined as follows:

$$\{p\}_{new} = \{p\}_{old} + \{\Delta p\} \tag{5}$$

The solution of Eq. (5) is obtained by an iterative procedure involving the simultaneous updating of the mass and/or the stiffness matrices and a resolution of the dynamic model for each iteration. The process is iterated until the results converge.

### *4.2 Weight matrix and definition of updating parameters*

The unknown parameters of the system are applied to each element as coefficients to define the changes in the structural characteristics. From a purely theoretical point of view, if a very large number of mode shapes are available, all the structural parameters can be modified with the same degree of reliability. However, in practice, the number of experimental mode shapes is measured at only a limited number of locations and over a limited frequency range. Consequently, some parameters will have very little or even nil influence on the experimental response. In order to overcome the problem of the incompleteness of the measured data, a weight matrix [$W$] is applied to assess the relative significance of the individual contributions. The updating parameter is expressed as follows:

$$\{\delta p\} = [W]\left([S]^T[S][W]\right)^{-1}[S]^T\{\delta w\} \tag{6}$$

In general, it is difficult to define the weight matrix; further, many cases demand an empirical evaluation. In order to determine the [$W$] matrix, it is necessary to analyse the ratio of the individual elements or macro elements to the mode shapes, as follows:

$$\xi_i = \frac{\{\phi_X\}^T[T]^T[K^e]_i[T]\{\phi_X\}}{\{\phi_X\}^T[T]^T[K][T]\{\phi_X\}} \tag{7}$$

where $X$ is an eigenvector of the experimental model; $[K^e]_i$, the stiffness matrix of the $i$-th macro element or element and [$T$], the system's reduction transformation.

Under the assumption that $m$ experimental vibration modes are available, the weight for each parameter can be given as follows:

$$W_{ii} = \frac{\sum_{j=1}^{m}\xi_{i,j}}{\max(W_{ii})} \tag{8}$$

Matrix [$W$] considers both the structural sensitivity of the elements and their influence on the experimental mode shapes; hence, it is very useful in the selection of the updating parameters.

### 4.3 Finite element model

The FE (finite element) model is composed of 83 macro elements that comprise 8-node isoparametric solid elements (Fig. 5). In other words, the FE model is composed of the arches, spandrels, full materials, buttresses, abutments and piers. The arch are divided into four in length and three in width, the spandrels are divided into four according to length and the piers are divided into five on the basis of height. From the material tests, the Young's moduli of the stone and the mortar are estimated to be 17.2 kN/mm$^2$ and 5.5–7.8 kN/mm$^2$, respectively (Aoki et al. 2004a). The Young's moduli of the arch, spandrel wall and pier depend on the thickness of the mortar, and are expected to be the same and/or larger than that of the mortar, but less than that of the stone. In the present analysis, their Young's modulus is assumed to be 7.8 kN/mm$^2$. On the other hand, the Young's modulus of the fill material is expected to be less than that of the mortar. Here, its Young's modulus is assumed to be 1/10 of that of the mortar, that is, 0.78 kN/mm$^2$. The specific gravity is assumed to be 1.83. The total number of nodes and elements is 6716 and 4552, respectively. The boundary condition of the two piers and both abutments is assumed to be fixed. From the results of preliminary model composed of 24 macro elements, since the stiffness of the fill materials is almost constant, the stiffness of the fill materials in this model is assumed to be constant.

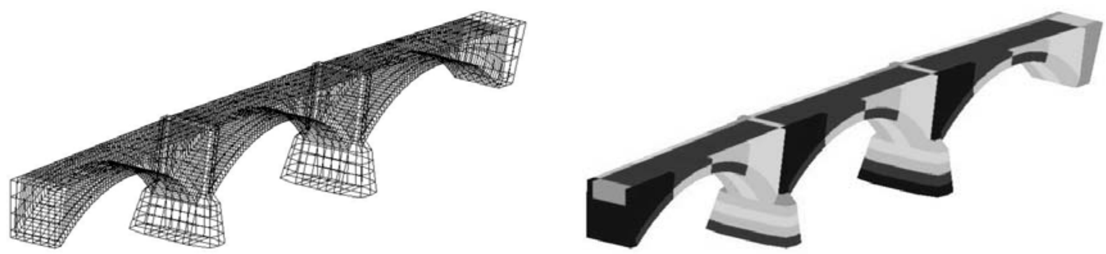

(a) FE model composed of 8-node solid elements (b) FE model of 83 macro elements

Figure 5 : Analytical model view from upstream side

### 4.4 Results of numerical model updating

The correction procedure uses experimental frequencies and mode shapes obtained from dynamic identification. As described in section 3.2, five principal modes in the vertical direction are determined by experimental measurements and dynamic identification. However, four experimental modes are used here for each FE model because there is a difficulty to compare the fifth experimental mode with the analytical one.

Fig. 6 shows the development of frequencies error and MAC (modal assurance criteria) in the iterative computation of the model. The influence of the experimental mode shapes is estimated by using the weight coefficients shown in Fig. 7. There is a difference between the initial and updated models. Table 2 shows the results of numerical model updating by a comparison of the initial mode parameters with the updated ones. Since the initial FE model is excessively idealized, errors of up to 11.7% between the measured and estimated frequencies obtained by the FE model are significant. The MAC between the measured and analytical modes of the updated model is approximately 1.0 for the second to fourth modes. After updating, the differences between the experimental and analytical frequencies are less than 0.96% for all the modes.

Table 2 : Results of numerical model updating

| State | Mode | Frequency (Hz) | | Error | MAC |
|---|---|---|---|---|---|
| | | Experimental | Analytical | (%) | |
| Initial Model | 1st | 7.900 | 7.936 | 0.45 | 0.418 |
| | 2nd | 9.180 | 9.147 | -0.36 | 0.936 |
| | 3rd | 11.020 | 10.083 | -0.85 | 0.811 |
| | 4th | 11.890 | 10.505 | -11.65 | 0.879 |
| Updated Model | 1st | 7.900 | 7.854 | -0.58 | 0.871 |
| | 2nd | 9.180 | 9.253 | 0.80 | 0.975 |
| | 3rd | 11.020 | 10.914 | -0.96 | 0.991 |

| | | | | |
|---|---|---|---|---|
| 4th | 11.890 | 11.939 | 0.42 | 0.968 |

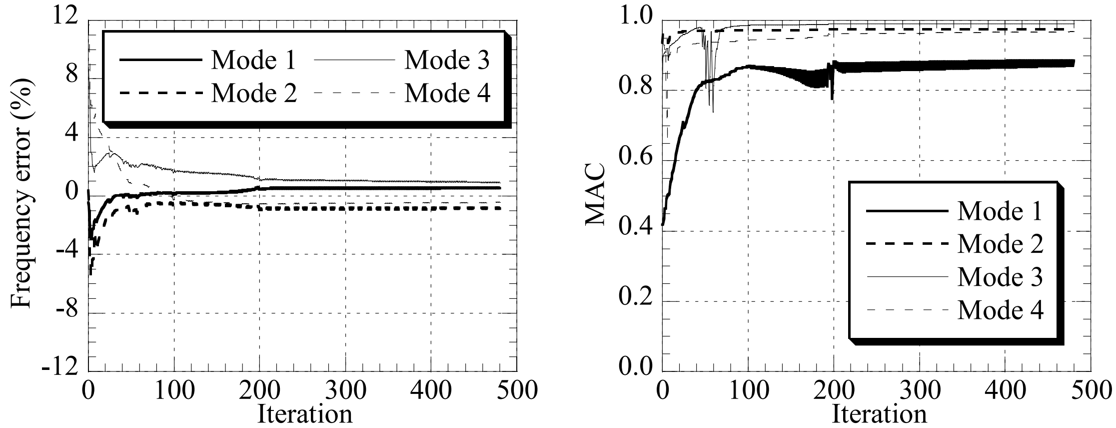


(a) Frequencies error (b) MAC

Figure 6 : Development of frequencies error and MAC in iterative computation

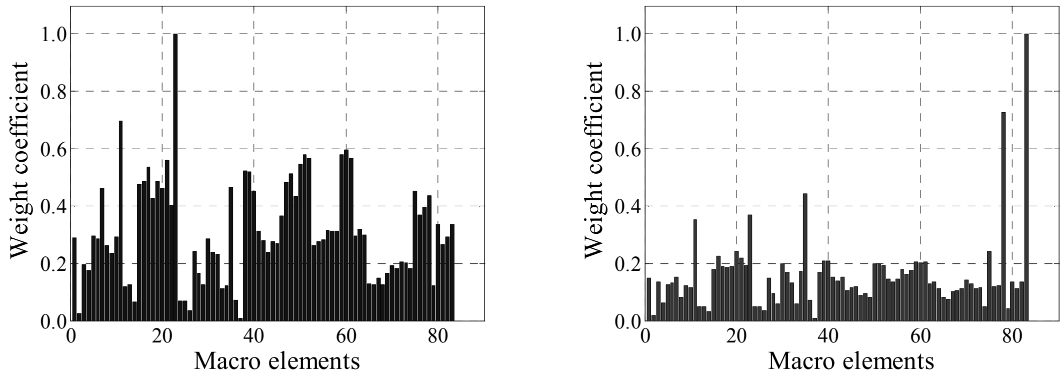


(a) Initial model (b) Updated model

Figure 7 : Weight coefficient of initial and updated models

With the model updated according to the experimental measurements, it is possible to determine the variations in the stiffness of the structural elements, as illustrated graphically in Fig. 8. This figure shows the stiffness correction coefficient $b_i$ associated with each macro element of the model. The stiffness correction coefficients obtained from updating the model using the mode shapes determined from the experimental measurements are also illustrated graphically in Figs. 8b and 8c. Based on the results of the numerical updating of the model, the stiffness of the three arch stones is increased, while the stiffness of the two piers is reduced. From the results of the numerical model updating, the following can be inferred:

1. The stiffness of the all macro elements at the arch stones is increased. Especially their stiffness near the piers and abutments increase almost two time of that of the initial model to simulate the increased arch thickness because they are not considered in the FE model.
2. The stiffness of the macro elements at the abutments and spandrels near the abutments is reduced probably due to the effect of the boundary condition.
3. The stiffness of the macro elements at other spandrels is increased to simulate the possible behaviour of the concrete slab because they are not considered in the FE model.
4. The stiffness of the macro elements at the piers is reduced probably due to the effect of bridge-soil interaction.
5. The stiffness of the macro elements at the spandrels near the piers is reduced probably due to the effect of cracks.

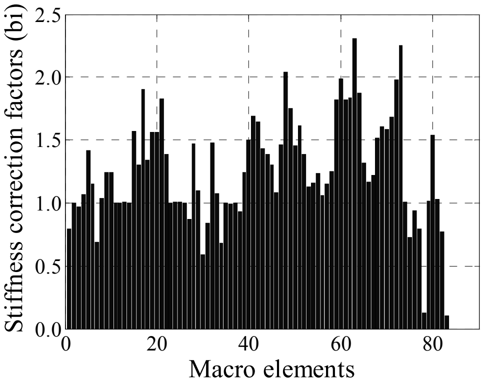


(a) Stiffness correction coefficients

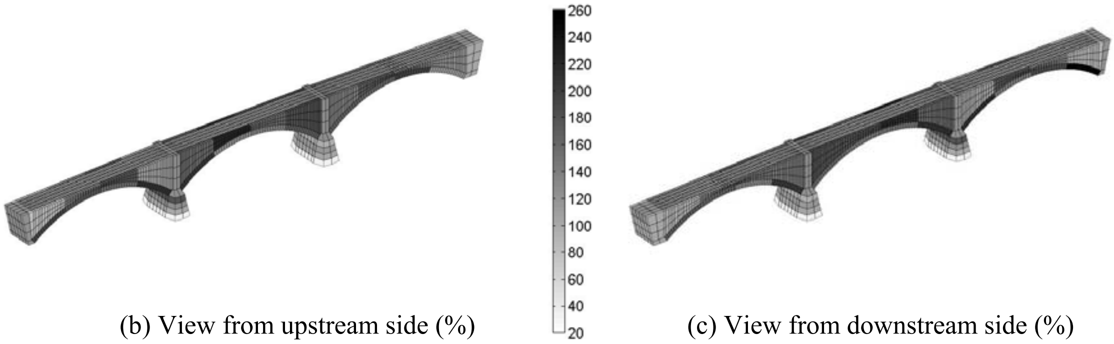


(b) View from upstream side (%) (c) View from downstream side (%)

Figure 8 : Stiffness correction coefficients obtained from model updating

Table 3 shows the experimental mode shapes identified by the ERA model and analytical ones of the initial and updated models.

Table 3 : Comparison between experimental, initial and updated mode shapes

| Experimental | Theoretical (Initial model / Updated model) |
|---|---|
| 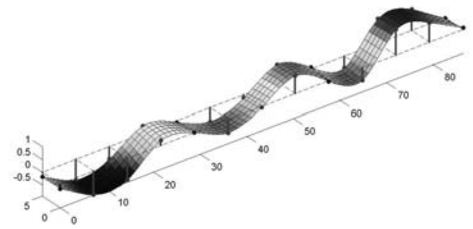 7.90Hz | 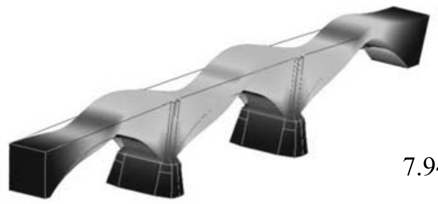 7.94Hz <br> 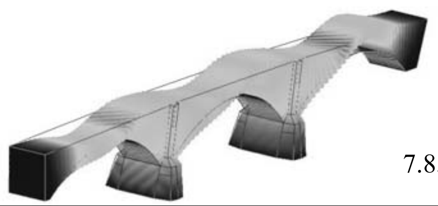 7.85Hz |
| 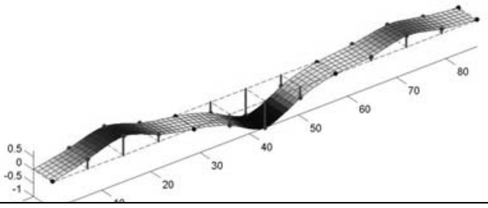 | 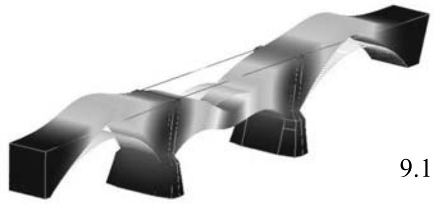 9.15Hz |

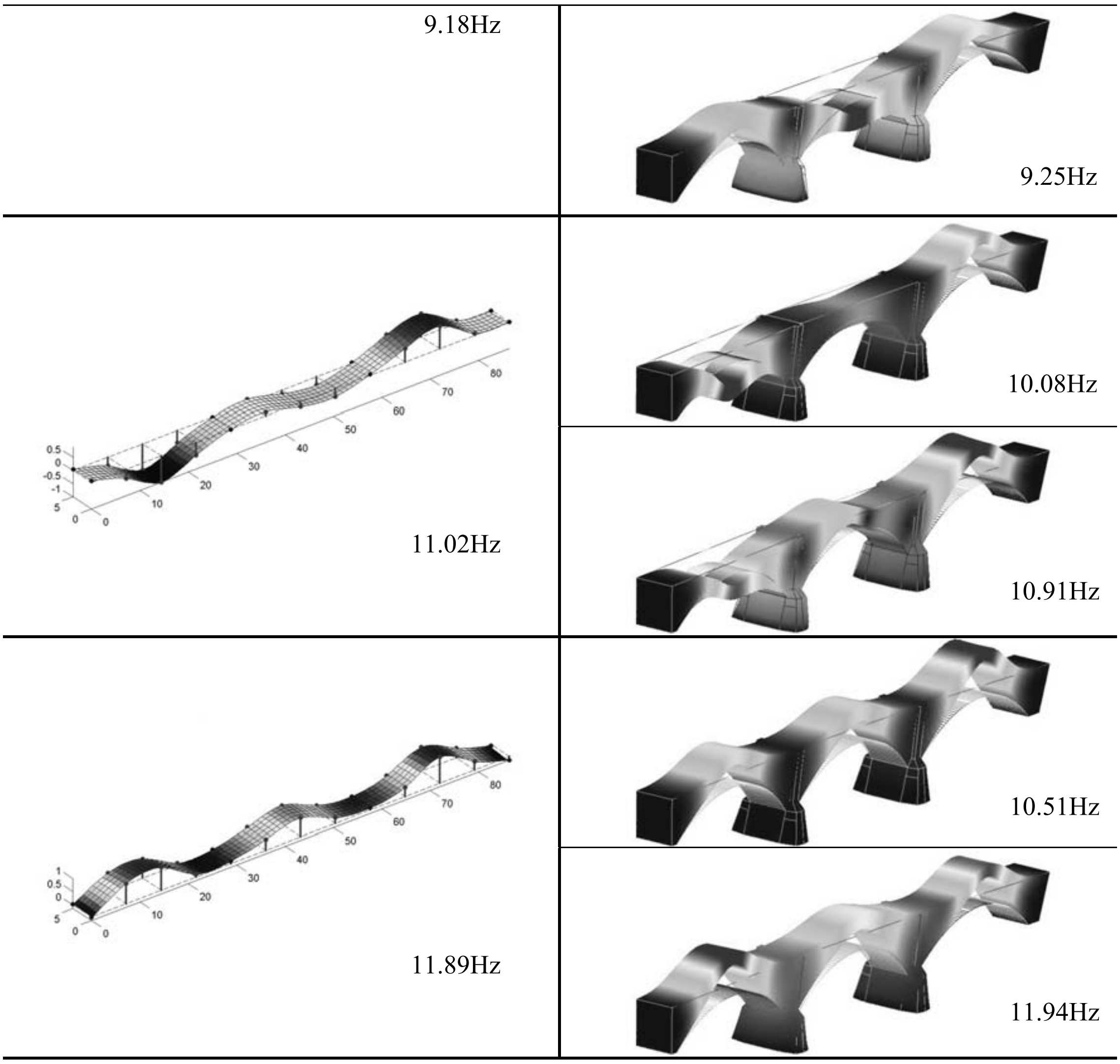


## 5 CONCLUDING REMARKS

The conclusions derived are as follows.

1) From the results of dynamic tests, the fundamental frequencies of the Rakanji stone arch bridge are estimated to be about 5.3 Hz and 7.6 Hz in the out-of-plane and vertical directions, respectively.
2) Variations in the stiffness characteristics of the Rakanji stone arch bridge (increase and decrease) are identified based on inverse eigensensitivity model updating. These results correspond well with the results obtained from investigation (Aoki et al. 2004a).

The obtained numerical updated model can simulate the real behavior of the Rakanji stone arch bridge and allow the evaluation of possible seismic performance, strengthening operation and the structural stability.

## ACKNOWLEDGEMENTS

Financial support was provided by Grants-in-Aid for Scientific Research (Kakenhi) and The Grant-in-Aid for Research from Nagoya City University.

## REFERENCES

Aoki, T., Komiyama, T., Miyata, S., Miura, M. and Igarashi, Y. 2004a. Research on deterioration for Rakanji stone arch bridge, Honyabakei, Oita, Japan. In P. Roca and C. Molins (eds.), *Arch bridge IV, Advances in assessment, structural design and construction*, p. 202-210. Barcelona: CIMNE.

Aoki, T., Komiyama, T., Sabia, D. and Rivella, D. 2004b. Theoretical and experimental dynamic analysis of Rakanji stone arch bridge, Honyabakei, Oita, Japan. *Proc. of 7th intern. conf. on motion and vibration control MOvIC'04, St. Louis, 8-11 August, 2004*, p. 1-9 in CD-ROM.

Friswell, M. I. and Mottershead, J. E. 1995. *Finite element model updating in structural dynamics*. Dordrecht: Kluwer Academic Publishers.

Juang, J. N. and Pappa, R. S. 1985. An eigensystem realization algorithm for modal parameter identification and model reduction. *Journal of Guidance, Control and Dynamics* 8(5), p. 620-627.

Jung, H. and Ewins, D. J. 1992. Error sensitivity of the inverse eigensensitivity method for model updating. *Proc. of 10th intern. modal analysis conf., San Diego, 3-7 February, 1992*, 2, p. 992-998